Agricultural and Forest Meteorology 331 (2023) 109321

Contents lists available at ScienceDirect

Agricultural and Forest Meteorology

journal homepage: www.elsevier.com/locate/agrformet

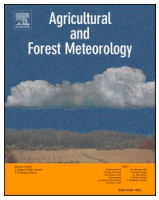

Climate variability and simultaneous breadbasket yield shocks as observed in long-term yield records

Weston Anderson [a,b,*], Walter Baethgen [a,*], Fabian Capitanio [c], Philippe Ciais [d], Benjamin I. Cook [e,f], Cunha G.R. da Cunha [g], Lisa Goddard [a,1], Bernhard Schauberger [h,i], Kai Sonder [j], Guillermo Podestá [k], Marijn van der Velde [l], Liangzhi You [m,n,*]

[a] International Research Institute for Climate and Society, The Earth Institute, Columbia University, New York, NY, United States
[b] Earth System Science Interdisciplinary Center, The University of Maryland, College Park, MD, United States
[c] Department of Veterinary Medicine and Animal Production, University of Naples Federico II, Naples, Italy
[d] Laboratoire des Sciences du Climat et de l'Environnement, LSCE/IPSL, CEA-CNRS-UVSQ, Université Paris-Saclay, Gif-sur-Yvette, France
[e] NASA Goddard Institute for Space Studies, New York, NY, United States
[f] Lamont-Doherty Earth Observatory, Palisades, NY, United States
[g] Brazilian Agricultural Research Corporation, Embrapa, Passo Fundo, RS, Brazil
[h] University of Applied Sciences Weihenstephan-Triesdorf, Freising, Germany
[i] Potsdam Institute for Climate Impact Research (PIK), Potsdam 14473, Germany
[j] International Maize and Wheat Improvement Center, Texcoco, Mexico
[k] Rosenstiel School of Marine and Atmospheric Sciences, University of Miami, United States of America
[l] European Commission, Joint Research Centre, Ispra 21027, Italy
[m] Macro Agriculture Research Institute, College of Economics and Management, Huazhong Agricultural University, Wuhan, Hubei 430070, China
[n] International Food Policy Research Institute, Washington, DC 20005, United States of America

ARTICLE INFO

Keywords:
Climate variability
Multiple breadbasket failures
Maize and wheat yield
El Niño Southern Oscillation
North Atlantic oscillation
Indian Ocean Dipole

ABSTRACT

That climate variability and change can potentially force multiple simultaneous breadbasket crop yield shocks has been established. But research quantifying the mechanisms behind such simultaneous shocks has been constrained by short records of crop yields. Here we compile a dataset of subnational crop yields in 25 countries dating back to 1900 to study the frequency and trends in multiple breadbasket yield shocks and how large-scale climate anomalies on interannual timescales have affected multiple breadbasket yield shocks over the last century. We find that major simultaneous breadbasket yield shocks have occurred in at least three, four, or five of nine breadbaskets 10.3%, 2.3% and 1.1% of the time for maize and 18.4%, 4.6% and 2.3% of the time for wheat. Furthermore, we find that multiple breadbasket yield shocks decreased in frequency even as those breadbaskets experience increasingly frequent climate-related shocks. For both maize and wheat breadbaskets, there were fewer simultaneous yield shocks during the 1975–2017 time period as compared to 1931–1975. Finally, we find that interannual modes of climate variability - such as the El Niño Southern Oscillation (ENSO), the Indian Ocean Dipole (IOD), and the North Atlantic Oscillation (NAO) - have all affected the relative probability of simultaneous yield shocks in pairs of breadbaskets by up to 20–40% in both maize and wheat breadbaskets. While past literature has focused on the effects of ENSO, we find that at the global scale the NAO affects the overall number of wheat yield shocks most strongly despite only affecting northern hemisphere breadbaskets.

1. Introduction

In recent decades international trade has become an increasingly important part of the global food system, with a majority of people now depending on food imports to meet daily caloric requirements (Porkka et al., 2013; Puma et al., 2015). Domestic food supply in heavily import-dependent countries is not always less stable than those that grow a larger fraction of their food (Bren d'Amour and Anderson 2020)

Abbreviations: ENSO, El Niño Southern Oscillation; IOD, Indian Ocean Dipole; NAO, North Atlantic Oscillation.

* Corresponding authors.
E-mail addresses: Weston@umd.edu (W. Anderson), Baethgen@iri.columbia.edu (W. Baethgen), L.YOU@mail.hzau.edu.cn (L. You).

[1] Deceased

https://doi.org/10.1016/j.agrformet.2023.109321
Received 12 August 2022; Received in revised form 10 January 2023; Accepted 13 January 2023
Available online 21 January 2023

as trade can either create conditions of food supply instability (Bren d'Amour et al., 2016) or lead to greater stability (Lybbert et al., 2014) depending on the context. But reliance on global food trade does present the unique risk that production shocks in remote countries can lead to reduced availability of food, which can contribute to price spikes that make food unaffordable (Bren d'Amour et al., 2016, Heslin et al., 2020, Marchand et al., 2016, Puma et al., 2015). In this context, the possibility of multiple simultaneous breadbasket yield shocks presents a potential risk to food security by limiting options for import diversification and raising the risk of export restrictions (Gaupp et al., 2020; Gaupp et al., 2019; Janetos et al., 2017, Mehrabi and Ramankutty, 2019, Tigchelaar et al., 2018, Toreti et al., 2019).

Large-scale modes of interannual climate variability - such as the El Niño Southern Oscillation (ENSO), the Indian Ocean Dipole (IOD), and the North Atlantic Oscillation (NAO)- are plausible mechanisms capable of affecting crop yields in multiple breadbaskets simultaneously (Anderson et al., 2020; W. 2019, 2018; Iizumi et al., 2014; Najafi et al., 2020; Singh et al., 2018). ENSO, the IOD, and the NAO refer to naturally occurring modes of climate variability in the ocean and atmosphere that affect atmospheric circulation, surface temperature, and precipitation on regional-to-global scales. These modes of climate variability, therefore, connect the growing conditions of distant regions and seasons to one-another (Anderson et al., 2018). While the potential for these climate modes to affect crop yields in multiple breadbaskets at once has been established using a few case studies (Anderson et al., 2019; Singh et al., 2018), the importance of this mechanism to multiple breadbasket yield shocks as compared to those forced by random weather or non-climate factors is still poorly understood. A primary reason is that to date, research on multiple climate-forced breadbasket yield shocks has been limited by short statistical records of 38–47 years (Gaupp et al., 2020; Kornhuber et al., 2020; Mehrabi and Ramankutty, 2019; Tigchelaar et al., 2018) as noted in a recent review on multiple breadbasket failures (Hasegawa et al., 2022). Modes of climate variability such as ENSO, however, are complex phenomenon (Timmerman et al., 2018) that vary on interdecadal timescales in terms of amplitude and return-period (Wittenberg, 2009). The length of records used by previous analyses, therefore, is insufficient to quantify the observed effects of these modes of variability on multiple breadbasket failures or to remove their potentially confounding effects from an analysis of observed historical trends (Hasegawa et al., 2022).

Our analysis addresses this constraint by collating a century-long maize and wheat yield dataset to provide the most complete picture to date of multiple breadbasket yield shocks, including observed trends and how climate modes have affected them. We compile a dataset of subnational crop yield anomalies for maize and wheat consisting of over 34,000 observations from 132 subnational units in 25 countries dating back to 1900 (Fig. 1), which we use to robustly estimate (1) the probability of multiple breadbasket yield shocks, (2) changes to that probability over the last century, and (3) to characterize how interannual modes of climate variability have affected the probability of such yield shocks in the historical record. The results presented here represent the most comprehensive assessment to date of the historical risk posed by climate variability to multiple maize and wheat breadbasket yield shocks.

2. Materials and methods

2.1. Data

Crop yield data are taken from the Twentieth Century Crop Statistics Data Set version 1, from which we use 34,000 observations from 132 subnational units in 25 countries dating back to 1900 (Anderson et al., 2022). The data used in this analysis are crop statistics at the subnational and national level, largely collected by national statistics agencies or departments and ministries of agriculture. Some of the data used has been previously analyzed, such that of Austria, Croatia, Czech Republic, and Belgium (Trnka et al., 2016), subnational data in France (Schauberger et al., 2018, 2022; Ceglar et al., 2020), Subnational data in southern Brazil (Cunha et al., 1999), and data in Argentina (Podestá et al., 1999), subnational data in Spain and Portugal (Páscoa et al., 2017), as well as multiple publications that have used the data in the United States, Australia, South Africa, and Canada. Other data was digitized from statistical yearbooks by Anderson et al. (2022), including the crop statistics from Italy, Spain, Indonesia, China, Mexico, Uruguay, Sweden, and Morocco. See SI Tables 3–4 for detailed information on the resolution and source of the statistics used in each country. No data on management was available for the full time period. To account for management trends that enabled higher yields over time we detrend the data.

Following past research identifying potentially damaging climate conditions relating to multiple breadbasket failures, we use temperature and moisture variables to identify damaging climate conditions (Gaupp et al., 2019; Zampieri et al., 2019). With the exception of (Zampieri et al., 2019), however, existing work on multiple breadbasket failures has often excluded moisture stress from the analysis (Tigchelaar et al., 2018; Kornhuber et al., 2020) or has focused on precipitation (Gaupp

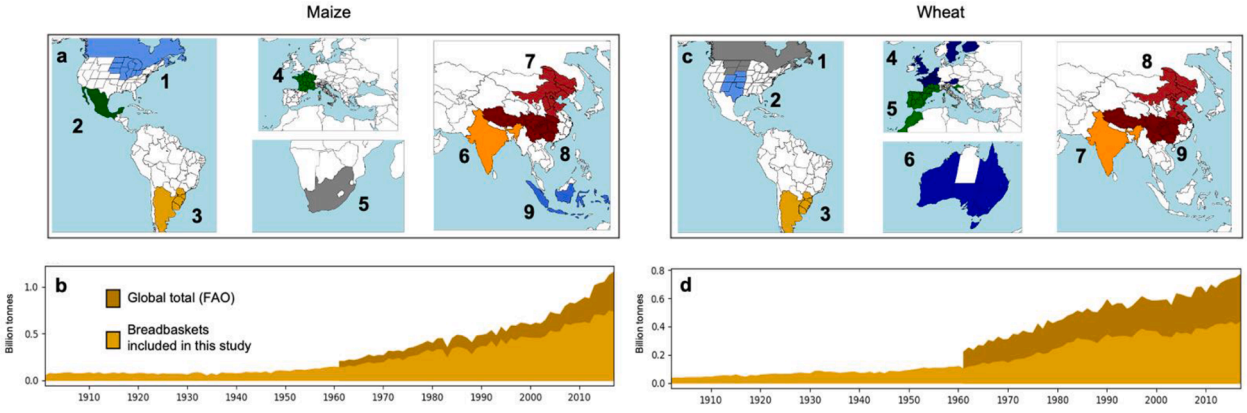

Fig. 1. Maize breadbasket regions included in this analysis (a) with breadbasket wheat-growing political units colored for: North America (1; NAm), Mexico (2; MEX), Southeast South America (3; SESA), Italy and France (4; ItFr), South Africa (5; SAf), India (6; IND), Northern China (7; NCh), Southern China (8; SCh), Indonesia (9; IDN). Total maize production included in the wheat breadbasket regions (light gold) compared to total global wheat production according to FAOSTAT (dark gold; b). Wheat breadbasket regions included in this analysis (c): Northern North America (1; NNAm), Southern United States Great Plains (2; USA), Southeast South America (3; SESA), Northern Europe (4; NEU), Mediterranean (5; MED), Australia (6; AUS), India (7; IND), Northern China (8; NCh), and Southern China (9; SCh). Total wheat production included in the wheat breadbasket regions (light gold) compared to total global wheat production according to FAOSTAT (dark gold; d).

et al., 2019; Kent et al., 2017; Sarhadi et al., 2018). Using precipitation rather than soil moisture as a measure of moisture supply, however, poorly captures the relationship between moisture supply and atmospheric moisture demand that leads to observed patterns of crop yield loss (Proctor et al., 2022; Rigden et al., 2020). To address this, we use hydroclimate variables that account for both supply and demand of moisture, including land surface model (LSM) based estimates of soil moisture from the Noah LSM in the Global Land Data Assimilation System (GLDAS) 2.0 over 1950–2009 (Rodell et al., 2004, 2013) and the self-calibrating Palmer Drought Severity Index (PDSI) for 1902 – 2017 (van der Schrier, 2013).

To calculate potentially damaging temperatures, we calculate both damaging maximum temperature and damaging minimum temperature during the crop growing season for maize and wheat in each location using the Berkeley Earth daily temperature dataset (Rohde 2013). Because crop yields respond nonlinearly to extreme heat (Schlenker and Roberts, 2009), we calculate extreme degree days (EDDs) as the sum of maximum temperatures exceeding an optimum threshold (29 °C for maize or 26 °C for wheat) over the growing season for each crop (Sanchez et al., 2014). Likewise, to calculate damaging minimum temperatures we calculate chilling degree days (CDDs) as the sum of daily minimum temperatures falling below an optimum threshold (8 °C for maize or 0 °C for wheat) over the growing season for each crop. Because crops may respond differently to these extreme temperatures in either very hot or very cold climates, however, we next convert both EDDs and CDDs to a z-score at the subnational level. In this way, we incorporate information about both baseline absolute temperature threshold exceedance and information on the frequency of such exceedance at the local scale.

Interannual modes of climate variability are assessed using the Niño 3.4 sea surface temperature (SST) index (5S-5 N and 170–120 W) and the Dipole Mode Index, which is the difference between western (50E-70E, 10S-10 N) and eastern (90E – 110E, 10S-0 N) Indian Ocean SSTs, both calculated by NOAA Physical Sciences Laboratory based on the HadISST1.1 dataset (Rayner et al., 2003), available for download at https://psl.noaa.gov/gcos_wgsp/Timeseries. The HadISST dataset uses a two-stage reduced-space optimal interpolation procedure, followed by a superposition of quality-improved gridded data. It improves on previous long reconstruction data in terms of SST mode variance and persistence through time. The North Atlantic Oscillation was identified using a station-based index, which, while noisier than an index derived from a full atmospheric pressure field, has the advantage of being defined by constant stations through time back to the mid-ninteenth century, thus eliminating the potential complication of changing observation systems (Hurrell et al., 1995).

2.2. Methods

2.2.1. Breadbasket yield shocks

To remove crop yield trends, we use the low-frequency Gaussian filter with a kernel density of five years, which is similar to the fifteen year running mean. We next convert yield anomalies at the subnational scale to percent anomalies by dividing the absolute yield anomalies by the expected yield. We define breadbaskets by identifying those countries that collectively contribute to 90% of maize or wheat production in 2010 and include all countries for which data is available. Based on these criteria, a total of 75% of maize production and 67% wheat production was available in our yield dataset from which we select breadbaskets that account for 66% and 58% of maize and wheat production, respectively. To decide how to define breadbaskets we consider average temperature and moisture regimes as an indication of agroclimate growing conditions. This procedure results in a total of nine breadbaskets for both maize and wheat. See SI Table 1 for the size of each breadbasket with respect to global total wheat or maize production in 2010, and SI Figure 1 for total production by breadbasket over time.

We aggregate the historical climate moisture availability and temperature stress variables to the subnational scale by averaging across the relevant crop growing seasons, defined using Sacks et al. (2010), and the subnational cropped region, defined as any cell having at least 10,000 ha of planted maize or wheat area as defined using the average of three estimates of crop extents: Portmann et al. (2010); You et al. (2014), and Fischer et al. (2001). The goal of this analysis is not to evaluate how breadbaskets have shifted over time, but rather to rigorously evaluate risks to present-day breadbaskets. As such, we aggregate absolute crop yield anomalies up to a time series of production anomalies for each breadbasket using static harvested area measurements averaged over 2005–2010 to represent present-day production systems. This results in a single time series for each breadbasket, which is converted to a percent yield anomaly as described earlier for the subnational and national-scale time series. For results using the historical dataset rather than static breadbaskets, which may be of interest with respect to the observed frequency of breadbasket yield shocks, see SI Figure 1.

Breadbasket failures have been defined either as the lower quartile of observed yield anomalies (Gaupp et al., 2020; Raymond et al., 2022) or as a 10% deviation from expected yields (Caparas et al., 2021; Tigchelaar et al., 2018). The lower quartile of yield anomalies in our breadbaskets generally corresponds to yield deficits of between ~5% and 10%. Accordingly, we define a yield shock at two thresholds: 5%, representing moderate yield shocks, and 10%, representing major yield shocks. Note that because we are using time-invariant harvested areas, our 10% yield threshold is equivalent to a 10% production threshold, which is the threshold used by Tigchelaar et al., (2018). Because a 10% threshold yields relatively few events, even in a century-long dataset, we additionally use the 5% threshold to be consistent with past literature and as an indication of moderate regional-scale yield deficits. Taken together, these two thresholds demonstrate the robustness of results.

To test whether the frequency of multiple breadbasket shocks have increased in the most recent period compared to earlier reporting periods we plot the probability density functions for the frequency of yield shocks in each period and use a two-tailed Kolmogorov-Smirnov test to evaluate whether the two distributions are statistically significantly different from one another. To remove the influence of World War I from our results, we exclude the years 1914–1919 in the Mediterranean and Europe breadbaskets. To remove the influence of World War II, we exclude the years 1940–1945 from the Mediterranean, Europe, India, and both North and South China breadbaskets.

To calculate the relative probability of joint yield shocks in pairs of breadbaskets and of multiple yield shocks globally during specific modes of interannual climate variability, we calculate the probability of an event occurring in each phase of the climate mode (e.g. ENSO, NAO, IOD) and difference the two (Fig. 2). See SI Table 4 for a list of years classified into each phase of each mode of variability using intensity thresholds of 0.5, 1.0, and 1.5 standard deviations. The probability of a yield shock occurring is calculated using a simple counting method as the number of years in which a major yield shock occurs in one breadbasket or multiple breadbaskets divided by the number of years included. The total subset of years in each case is constrained to be those years with a particular mode of variability active in a particular phase. While this approach is relatively simple, it leverages the long data record without making assumptions about the structure of the distribution or of the joint distribution.

To test for statistical significance, we adopt a bootstrap-based approach, which preserves the statistical properties of each breadbasket time series and takes into account the sample size (see SI Table 4) of each composite used to calculate probabilities of joint yield shocks in each phase of a given climate mode. To calculate the null hypothesis for each climate mode, we randomly draw n samples from each breadbasket time series without replacement, where n is the number of observed years in which the given climate mode is in a particular phase, and calculate the probability of joint yield shocks between each pair of breadbaskets. We repeat this process 1000 times to produce a

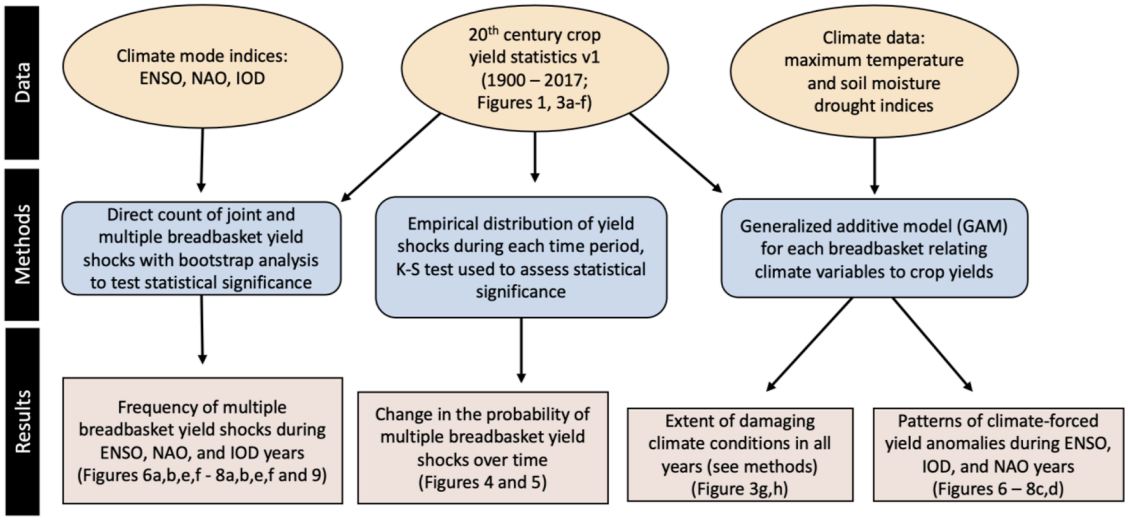

Fig. 2. Flowchart demonstrating the data, methods, and results of the analysis.

distribution for each calculated joint yield shock probability and identify the 5th and 95th percentiles of each to use to test statistical significance.

While decadal and multi-decadal climate variability may also affect crop yields (Schillerberg and Tian, 2020; Tian et al., 2015), our analysis focuses on interannual modes of climate variability. Quantifying the impacts that decadal climate variability has had on crop yields would require careful methodological consideration unique to the problem of decadal variability. As such, we do not consider modes such as the Atlantic Multidecadal Oscillation or the Pacific Decadal Oscillation, focusing instead on ENSO, the NAO, and the IOD.

2.2.2. *Breadbasket climate stress*

We aggregate the historical climate variables to the subnational scale using global cropping calendars and major cropped area, defined as any cell having at least 10,000 ha of planted maize or wheat area, before converting each time series to a z-score (see SI for details). We relate the climate stress covariates to the yield anomalies using a generalized additive model (GAM) for each breadbasket. We choose a GAM structure because it is a flexible, nonlinear model and as such can estimate climate conditions that would be damaging to yields due to both excess or deficit temperature, moisture, and their interaction (Hastie and Tibshirani, 2009). We restrict the complexity of each GAM model to include a maximum of five spline terms. We consider two bivariate tensor terms in each GAM, one for maximum temperature stress and moisture stress, and one for minimum temperature stress and moisture stress, such that each model is as follows:

$$Yld_{ikj} = s(SM_{ikj}) + te_1(KDD_{ikj}, SM_{ikj}) + te_2(CDD_{ikj},\ SM_{ikj}) + T_{jk}$$

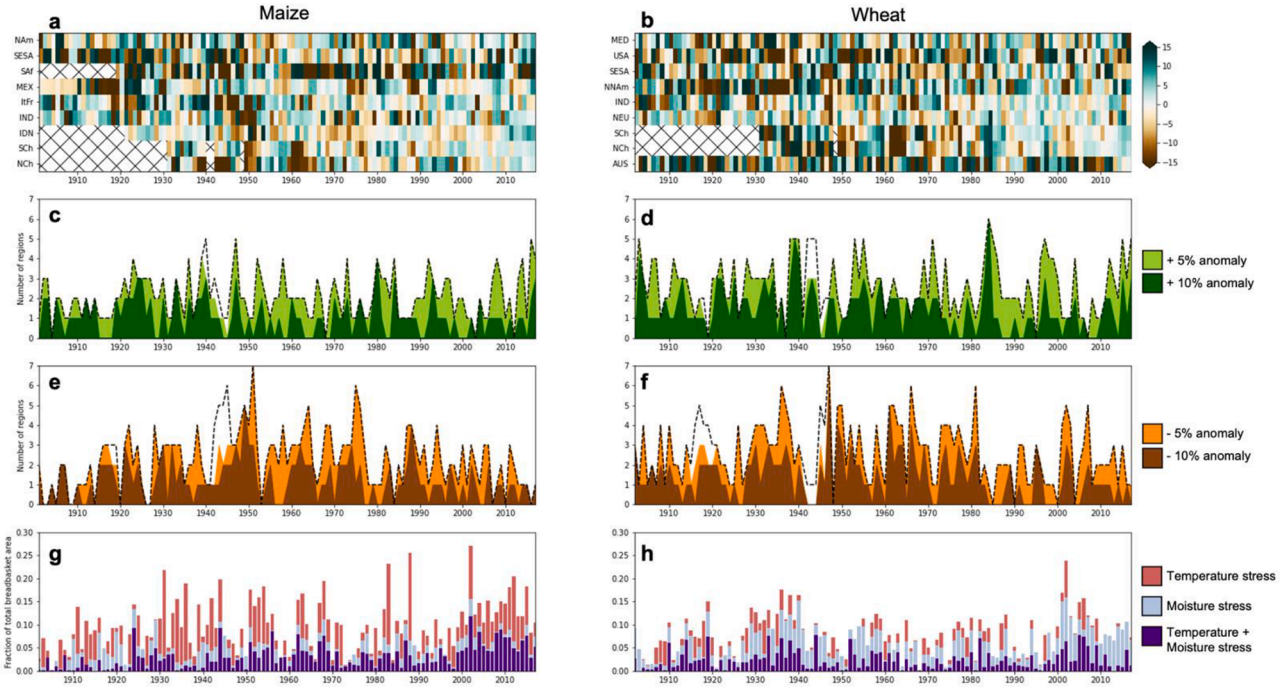

Fig. 3. Regional crop yield surplus and deficit exceedance curves. Exceedance probabilities for wheat (a) and maize (b) surpluses and deficits (e,f) of between 1\% and 10\% occurring simultaneously in between 0 and 8 breadbasket regions over the entire 1901–2017 time period. Difference between the probabilities of exceedance in the earliest period for which all regions report data (1931–1975) and the more recent period (1975–2017) for wheat (c) and maize (d) surpluses and deficits (g,h).

where Yld_{ikj} is the crop yield anomaly in national or subnational unit i from breadbasket k for year j, while KDD_{ikj}, CDD_{ikj}, and SM_{ij} represents the killing degree days, chilling degree days, and soil moisture anomalies in the national or subnational unit i from breadbasket k for year j that corresponds to the resolution of the crop yield data, and T_{jk} represents a time fixed effect for year j in breadbasket k. Note that the time fixed effect is only applied to breadbaskets containing more than one administrative unit. The function s() is a spline function while the functions $te_1()$, and $te_2()$ are tensor products, which serve as the multidimensional basis functions with restricted degrees of freedom, in this case five, to prevent over-fitting (Hastie et al., 2009). Constructing the GAM models using soil moisture information from the Noah land surface model or using PDSI yields similar results for the overlapping time period. We show results using the soil moisture model as data allows, which is everywhere except for Fig. 3, where information prior to 1950 is required and a PDSI-based model is used. See SI Section 3 for further details on the GAM model specification, fit, and evaluation. Climate conditions that are damaging in each breadbasket are identified as those that produce at least 10% yield deficits according to the GAM models fit for each breadbasket. By holding either temperature or moisture at average conditions but allowing the other variable to vary in time, we can isolate the effect of univariate climate stress as compared to bivariate stress. In the event that both univariate and bivariate climate stress produces damaging conditions at a particular point in space and time, the univariate stress indicator is used.

3. Results

We assess two yield anomaly magnitudes: a yield deficit of 10% relative to expected yields, which we will refer to as a major yield shock, and one at a 5%, which we will refer to as a moderate yield shock (see Methods). Note that the number of breadbaskets experiencing simultaneous yield shocks is closely related to total breadbasket production (SI Figure 3).

In nearly a century, major crop yield shocks tended to occur in two to three, but rarely more than three maize or wheat breadbaskets simultaneously (Fig. 3,ef). From 1930–2017 major yield shocks occurred in at least three, four, or five maize breadbaskets 10.3%, 2.3% and 1.1% of the time, respectively. Simultaneous major wheat yield shocks were nearly twice as common, occurring in three, four, or five breadbaskets 18.2%, 4.6%, and 2.3% of the time, respectively. Moderate yield shocks are more common, occurring more regularly in three to four maize or wheat breadbaskets. We characterize the complete probability profile of multiple breadbasket yield shocks and surpluses of magnitudes between 1% and 10% in Fig. 5. A major yield shock occurred in at least two maize or wheat breadbaskets 35–40% of the time, while a moderate yield shock occurred in at least two breadbaskets 68–72% of the time (Fig. 4 and Fig. 5c,d). Major wheat yield surpluses (+10%), on the other hand, occurred in at least two breadbaskets 43% of the time while major maize yield surpluses only simultaneously occurred in at least two breadbaskets 22% of the time.

Wheat and maize breadbasket yield shocks have not been increasing in frequency over the last hundred years, regardless of which yield threshold is used (Figs. 3 and 5). In fact, the number and prevalence of simultaneous maize and wheat shocks has been lower ($p<0.1$) at both the 5% and 10% yield threshold in recent decades (1975–2017) as compared to earlier decades (1931–1975). This is true regardless of whether the analysis is conducted for present-day static breadbaskets (Fig. 3e,f) or using breadbaskets with historical time-varying harvested areas (SI Figure 2). The statistical significance of the decrease in major yield shocks is robust to the definition of early and late periods, as well as to the decision to include World Wars 1 and 2 or the decision to include Northern China and India, which have experienced large changes in irrigated area (SI Figure 4, SI Tables 5 and 6). Only the 5% yield threshold for wheat is sensitive to the decision of excluding areas with a change in irrigation, indicating that for wheat breadbaskets

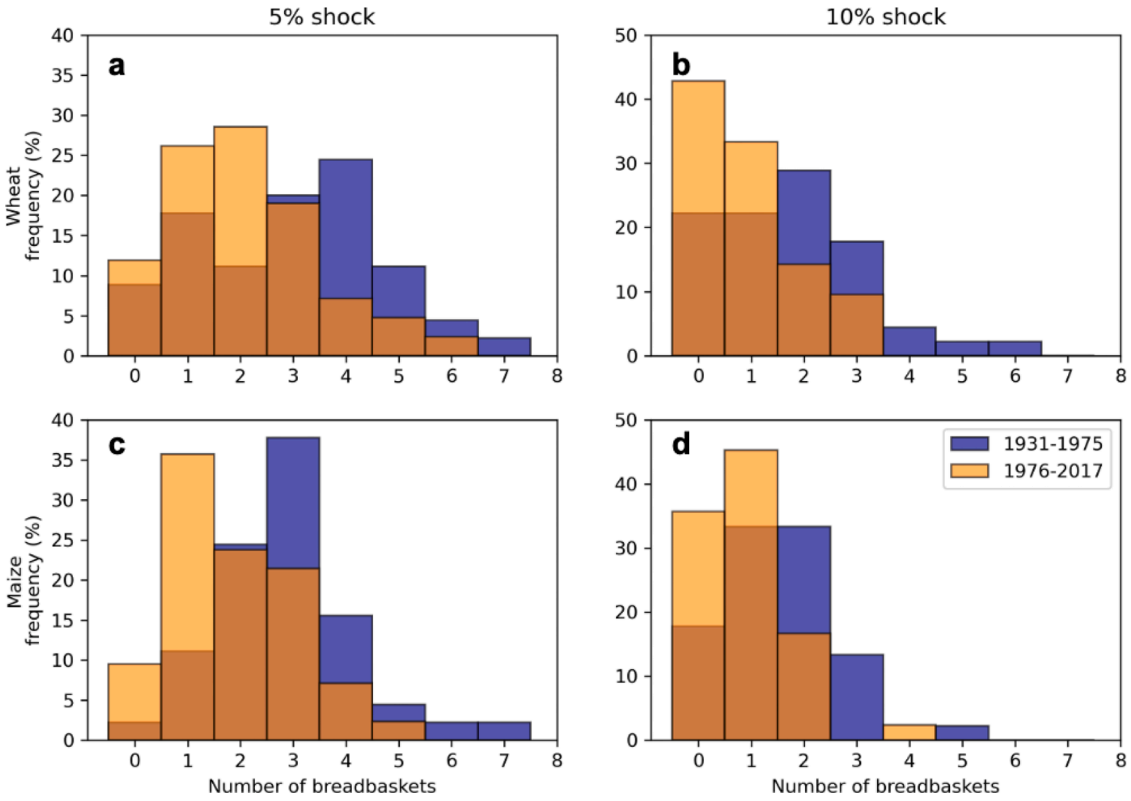

Fig. 4. Probability distribution functions for the frequency of having a yield shock in between one and eight breadbaskets simultaneously in the 1931–1975 period compared to the 1976–2017 period for maize and wheat at yield thresholds of 5% and 10%.

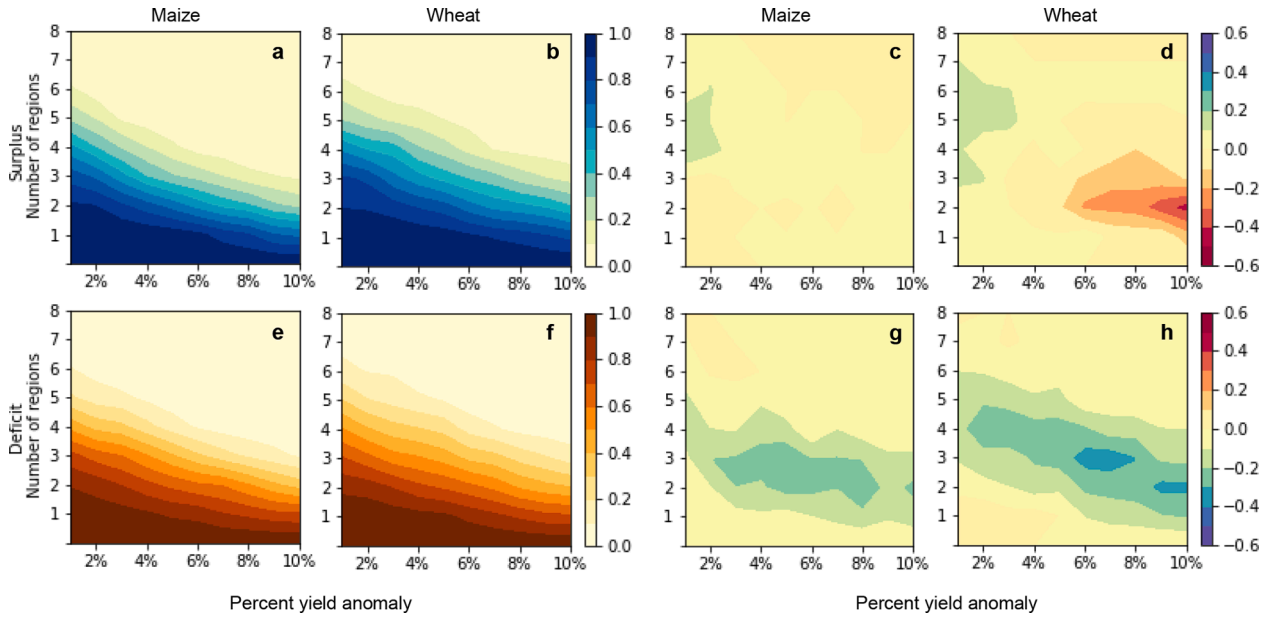

Fig. 5. Regional crop yield surplus and deficit exceedance curves. Exceedance probabilities for wheat (a) and maize (b) surpluses and deficits (e,f) of between 1% and 10% occurring simultaneously in between 0 and 8 breadbasket regions over the entire 1901–2017 time period. Difference between the probabilities of exceedance in the earliest period for which all regions report data (1931–1975) and the more recent period (1975–2017) for wheat (c) and maize (d) surpluses and deficits (g,h).

irrigation may have played a role in reducing the frequency of minor yield shocks. When comparing maize and wheat yield shocks at all yield anomaly magnitudes from the more recent period to those in the earlier period (Fig. 4), we find yield shocks occurring in 2–4 breadbaskets simultaneously became up to 30% less frequent. Simultaneous maize yield surpluses, on the other hand, have remained constant while simultaneous wheat yield surpluses of greater than 5% have decreased. See SI Figures 5–6 for the 1975–2010 and 1931–1975 return periods for maize and wheat.

The decline in the frequency of crop yield shocks in breadbasket areas is observed despite an increase in the frequency of damaging climate stress in breadbasket areas, particularly after the year 2000

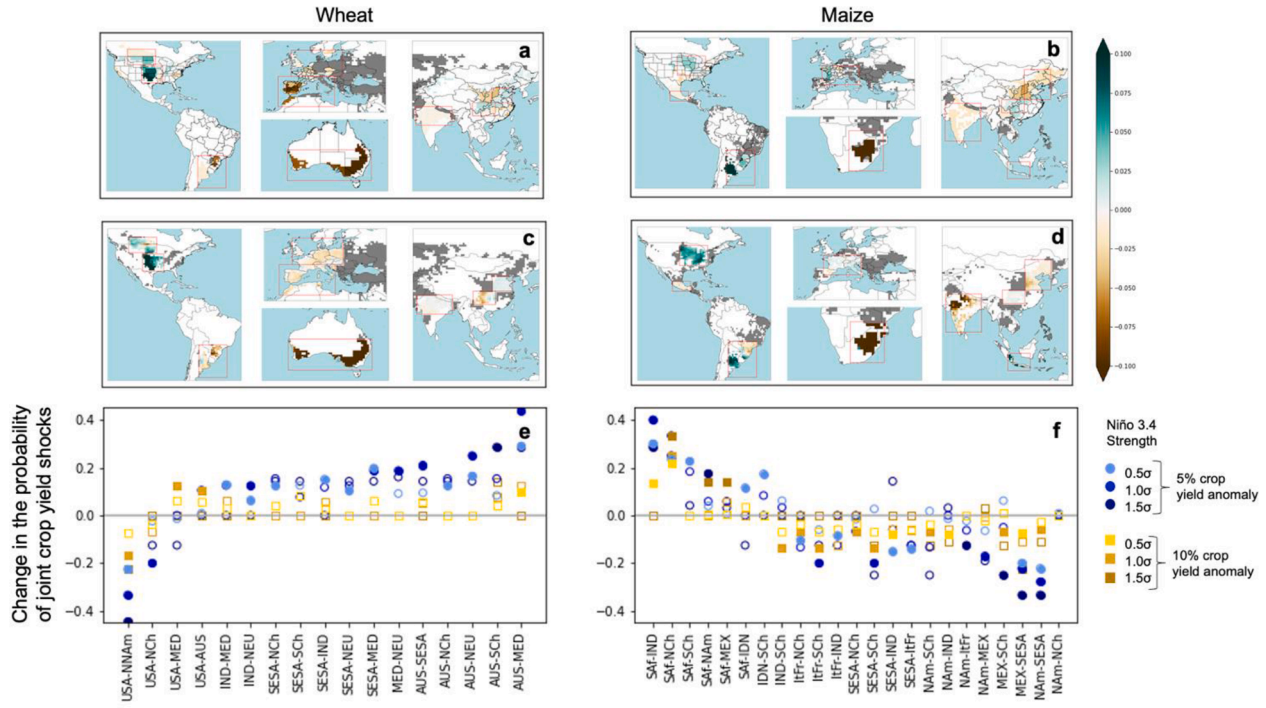

Fig. 6. Probability of joint crop yield shocks in breadbasket regions during ENSO events. Observed fractional wheat (a) and maize (b) yield anomalies during 1$ \sigma$ strength El Ni\~{n}os as compared to La Ni\~{n}as events. Climate-forced fractional wheat (c) and maize (d) yield anomalies (see methods) during El Ni\~{n}o as compared to La Ni\~{n}a events. Difference in the probability of joint wheat (e) and maize (f) yield shocks for pairs of breadbasket regions during El Ni\~{n}o as compared to La Ni\~{n}a. Shading intensity for each point signifies ENSO event definition using a standard deviation threshold of 0.5, 1.0, or 1.5. Only pairs of regions with statistically significant points (p$<$0.05 based on a bootstrap test for significance, see Methods) are shown. USA-Northern China pair is additionally included for maize. Filled symbols indicate statistical significance, unfilled symbols indicate that differences were not significant at the 95\% level.

(Figs. 3 g, h). In addition to the post-2000 increase in climate shocks, there is decadal variability in the extent of damaging climate stress. Comparing the widespread frequency of damaging climate conditions affecting wheat and maize breadbaskets in the 1930s and 1940s to the relatively low levels in the 1960s and 1970s makes clear that both decadal variability and long-term climate change affect the incidence of dry and hot anomalies in breadbasket areas. This is consistent with the findings of Lesk and Anderson (2021), and highlights the importance of considering both natural variability and climate change as a potential driver of climate-related yield shocks.

3.1. *Climate-drivers of multiple breadbasket shocks*

The general lack of widespread breadbasket yield shocks in Figs. 3–5 lends credibility to the notion that producing crops in breadbaskets with relatively uncorrelated risks buffers against the probability of multiple simultaneous crop yield shocks. However, as pointed out by Anderson et al. (2019), global modes of climate, such as the El Niño Southern Oscillation (ENSO), may affect the climate in such a way that increases the likelihood of these simultaneous crop yield shocks relative to other years.

Using our century-long yield dataset, we find that modes of climate variability have had a large effect on the probability of joint yield shocks in pairs of breadbaskets. The probability of joint yield shocks differs by up to 40% in opposite phases of major climate modes (Figs. 6–8). For both wheat and maize, the IOD and ENSO affect crop yields in a balanced manner, increasing the probability of joint yield shocks in some breadbaskets and reducing the probability of joint yield shocks elsewhere (Figs. 6–7). The North Atlantic Oscillation (NAO), however, exerts a unidirectional influence on the probability of joint wheat or maize breadbasket shocks, although its influence on maize is limited (Fig. 8).

El Niño events create damaging climate conditions for wheat relative to La Niña events in parts of Southeast South America due to excess precipitation (Anderson et al., 2018; Anderson et al., 2019; Cunha et al., 2001) and in the Mediterranean and Australia due to drought (Anderson et al., 2018: Yuan and Yamagata, 2015, Ummenhofer et al., 2009) (Fig. 6c). These adverse climate conditions reduce wheat yields in these breadbaskets (Fig. 6a) and increase the probability of joint wheat yield shocks between pairs of breadbaskets that include Australia, the Mediterranean, or Southeast South America by up to 20–40% with the strongest influence on the joint probability of moderate yield shocks in Australia and the Mediterranean. On the other hand, El Niños increase winter precipitation that leads to increased springtime soil moisture and improves wheat yields in the Great Plains of North America (Anderson et al., 2017a, 2018; Mauget and Upchurch, 1999), which decreases the probability of a joint wheat yield shock in these breadbaskets by up to 45%.

For maize, El Niños increase precipitation and reduce the incidence of damaging maximum temperatures relative to La Niñas in Southeast South America (Anderson et al., 2017a, 2018; Cunha et al., 2001; Podestá et al., 1999) and the US Midwest (Anderson et al., 2017a, 2017b; Handler 1984) (Fig. 6d), which translates into above-expected maize yields (Fig. 6b). El Niños, however, also force drought in South Africa (Anderson et al., 2019; Funk et al., 2018), India (Selvaraju et al., 2003), and Northern China (Liu et al., 2014), which translates to below-expected maize yields in these breadbaskets during El Niños relative to La Niñas (Fig. 6b). As a result of these teleconnections, El Niños tend to increase the probability of joint yield shocks in pairs of breadbaskets that include South Africa by 10–40%, most notably modifying the probability of joint yield shocks in South Africa and Northern China, and South Africa and India. However, El Niño teleconnections also tend to decrease the likelihood of joint maize yield shocks in pairs of breadbaskets that include Southeast South America or

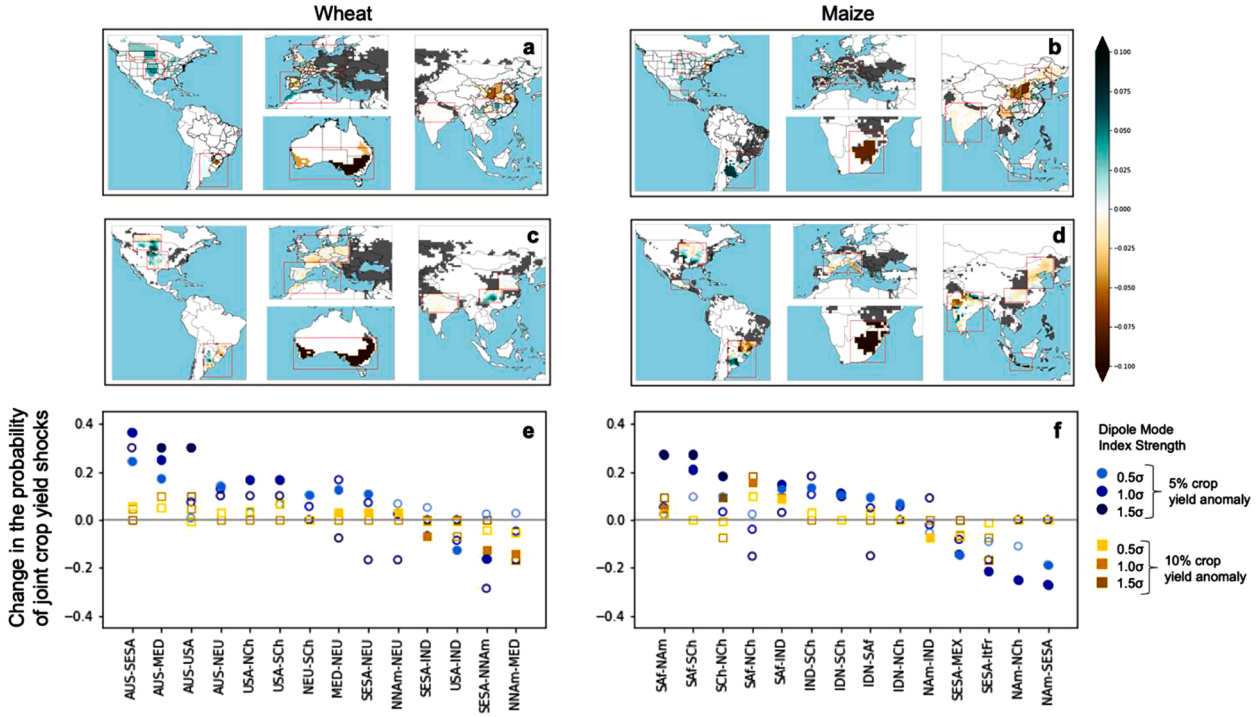

Fig. 7. Probability of joint crop yield shocks in breadbasket regions during IOD events. Observed fractional wheat (a) and maize (b) yield anomalies during 1$\sigma $ strength positive phases of the IOD as compared to negative phases. Climate-forced fractional wheat (c) and maize (d) yield anomalies (see methods) during positive phases of the IOD as compared to negative phase. Difference in the probability of joint wheat (e) and maize (f) yield shocks for pairs of breadbasket regions during positive phases of the IOD as compared to negative phase. Shading intensity for each point signifies IOD event definition using a standard deviation threshold of 0.5, 1.0, or 1.5. Only pairs of regions with statistically significant points (p$<$0.05 based on a bootstrap test for significance, see Methods) are shown. USA-Northern China pair is additionally included for maize. Filled symbols indicate statistical significance, unfilled symbols indicate that differences were not significant at the 95\% level.

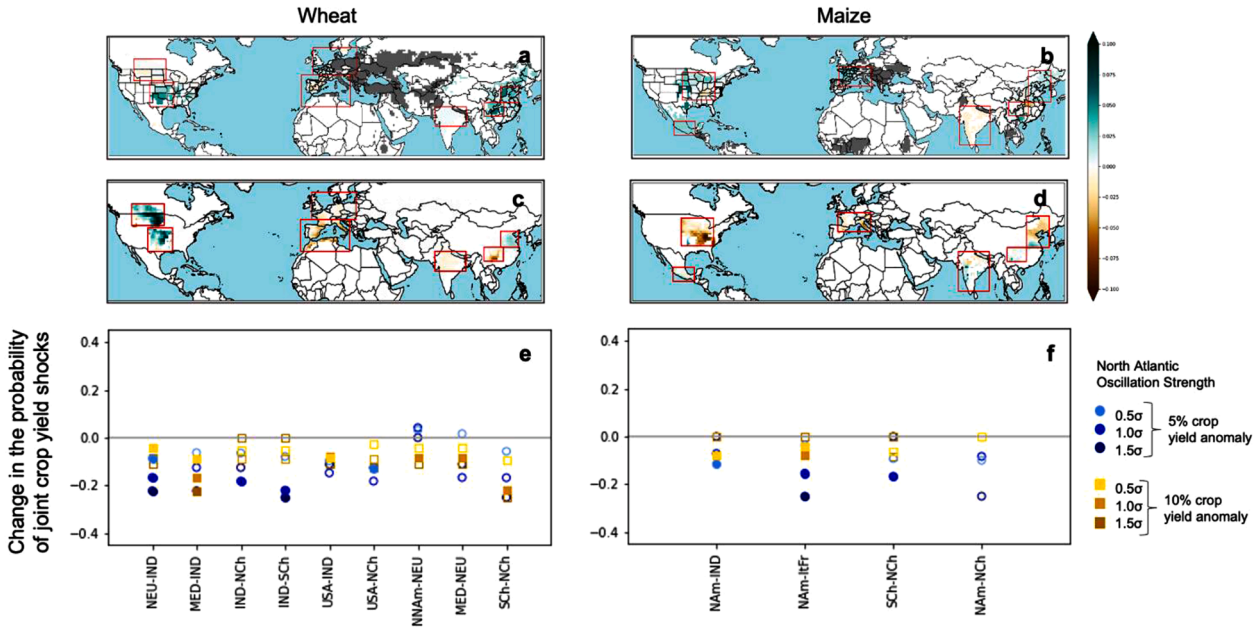

Fig. 8. Probability of joint crop yield shocks in breadbasket regions during NAO events. Observed fractional wheat (a) and maize (b) yield anomalies during 1$ \sigma$ strength positive phases of the NAO as compared to negative phases. Climate-forced fractional wheat (c) and maize (d) yield anomalies (see methods) during positive phases of the NAO as compared to negative phase. Difference in the probability of joint wheat (e) and maize (f) yield shocks for pairs of breadbasket regions during positive phases of the NAO as compared to negative phase. Shading intensity for each point signifies NAO event definition using a standard deviation threshold of 0.5, 1.0, or 1.5. Only pairs of regions with statistically significant points (p$<$0.05 based on a bootstrap test for significance, see Methods) are shown. USA-Northern China pair is additionally included for maize. Filled symbols indicate statistical significance, unfilled symbols indicate that differences were not significant at the 95\% level.

Northern North America by ~10–35%. Of particular relevance to global maize production are the offsetting ENSO teleconnections in Northern North America and Northern China (see Anderson et al., 2018), such that the probability of a joint yield shock in the two breadbaskets during ENSO events is unaffected.

The IOD has an effect similar, but not identical, to that of ENSO in many breadbaskets in terms of both climate stress and yield anomalies (Anderson et al., 2019; Chan et al., 2008; Funk et al., 2018; Goddard et al., 1999; Liu et al., 2014, Yuan and Yamagata, 2015) although it has less of an influence on climate and crop yields in North America and Europe (Fig. 7). Because of this, the effect the IOD has on the probability of joint yield shocks is statistically significant in fewer of the pairs of breadbaskets compared to ENSO, although it can still affect the probability of joint yield shocks in pairs of breadbaskets by up to ~30%. The strongest influence of the IOD on joint wheat yield shocks is between pairs of breadbaskets that include Australia, where a positive IOD increases the probability of drought and wheat failures in Southeast Australia (Yuan et al., 2015). For maize it most strongly affects the probability of joint crop yield shocks in pairs of breadbaskets that include South Africa, where a positive IOD increases the probability of drought (Funk et al., 2018; Goddard et al., 1999) that damages maize yields, and Southeast South America, where a positive IOD increases precipitation in Argentina (Chan et al., 2008), which is improves maize yields.

The NAO does not significantly affect as many breadbaskets as does ENSO or the IOD, but the direction of its influence is the same in all breadbaskets that it does affect (Fig. 8). Positive NAO events reduce the risk of frost kills and produce wet, mild winters that improve crop yields in North America and Northern Europe (Baek et al., 2017; Cantelaube et al., 2004; Maignan et al., 2008), mixed precipitation conditions in the North China Plain (Baek et al., 2017), and drought in the Mediterranean and India (Baek et al., 2017; Cantelaube et al., 2004; Lamb et al., 1987; Maignan et al., 2008). These teleconnections reduce the probability of joint wheat yield shocks in pairs of breadbaskets that include Northern China, the Southern Great Plains, and Northern Europe by ~10–25%, while negative NAO events increase the probability of joint wheat yield shocks in these breadbaskets. The NAO affects very few maize breadbaskets, although it does affect the probability of joint maize yield shocks in three pairs of breadbaskets, most notably the US Great Plains and Europe in the growing season following an NAO event.

When these regional probabilities are aggregated to the global scale, we find that the NAO and ENSO affect the probability of multiple breadbasket yield shocks by up to 30% and 40%, respectively, while the IOD has fewer statistically significant effects (Fig. 9). El Niños decrease the probability of over four simultaneous maize yield shocks as compared to La Niñas, but increase the likelihood of 2–3 simultaneous shocks, although the latter is not statistically significant. The negative phase of the NAO is most strongly associated with an increased probability of simultaneous wheat breadbasket shocks despite ENSO affecting a larger geographic area and a greater number of breadbaskets than does the NAO, which only affects the climate of the northern hemisphere. But the NAO either increases or decreases the likelihood of wheat shocks in all breadbaskets that it affects, depending on the phase, which is why at a global scale it affects the probability of multiple wheat breadbasket shocks more strongly than ENSO.

3.2. *Discussion and conclusions*

Using our century-long dataset of national and subnational crop yields, we find that simultaneous yield shocks in wheat and maize breadbaskets have been less frequent in recent decades as compared to mid-century. While damaging climate stress during maize and wheat growing seasons has increased in breadbasket areas after the turn of the century, - particularly the incidence of joint moisture-temperature stress for maize - the frequency of multiple simultaneous wheat and maize breadbasket yield shocks has decreased (see Figs. 3–5). These results are consistent with Gaupp et al. (2020) and Sarhadi et al. (2018), who found increases in the frequency of temperature- and precipitation-related risks across breadbaskets and agricultural areas, respectively, in recent decades. Our results, however, indicate that such risks have not yet

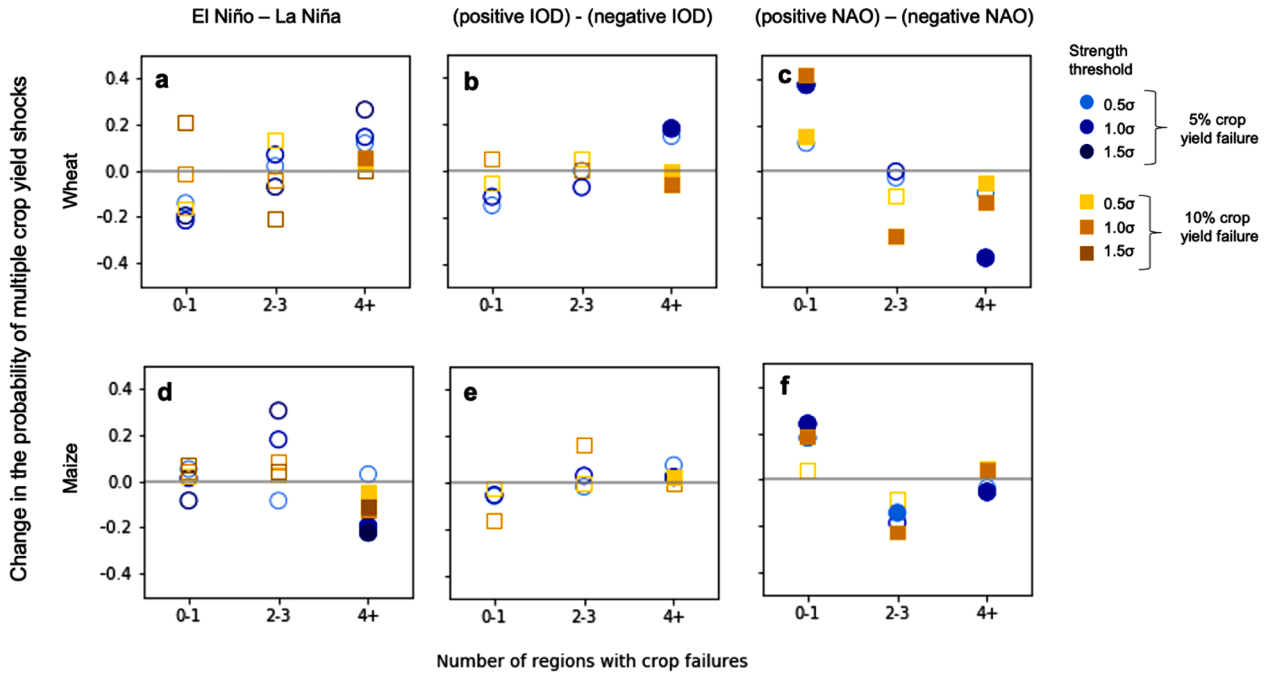

Fig. 9. Probability of multiple simultaneous crop yield shocks in breadbasket regions. Anomalous probability of zero-one, two-three, or over four wheat (a-c) and maize (d-f) breadbasket yield shocks during the positive phase as compared to the negative phase of ENSO (a,d), the IOD (b,e), and the NAO (c,f).

translated into substantially more frequent maize or wheat breadbasket yield shocks to date (Fig. 3).

Our results furthermore highlight the discrepancy between observed and expected trends in multiple breadbasket failures. As the climate continues to warm, we expect an increased frequency of hot-and-dry conditions to damage crop yields in major maize and some wheat breadbaskets (Caparas et al., 2021; Gaupp et al., 2019, 2020; Jägermeyr et al., 2021: Raymond et al., 2022: Sarhadi et al., 2018: Tigchelaar et al., 2018). In most wheat breadbaskets, average global yields are expected to continue to increase and stabilize due to the CO_2 fertilization effect despite warming temperatures (Caparas et al., 2021: Jägermeyr et al., 2021, Liu et al., 2019, 2021). The exception to the expected stability of wheat breadbaskets is India (Liu et al., 2019, 2021), where the combination of growing season temperature increases and constraints on irrigation are likely to make yields more variable and crop failures more common (Caparas et al., 2021; Jain et al., 2021; Liu et al., 2019, 2021). For maize breadbaskets, which will not greatly benefit from increased CO_2, increasing temperatures will lower global average yields, increase the frequency of crop yield shocks, and increase the frequency of multiple maize breadbasket failures (Caparas et al., 2021; Gaupp et al., 2020; Jägermeyr et al., 2021; Raymond et al., 2022; Tigchelaar et al., 2018). That the future instability of maize breadbaskets is well supported by multiple lines of evidence (e.g. using both statistical models (Raymond et al., 2022; Tigchelaar et al., 2018) and process based models (Caparas et al., 2021; Jägermeyr et al., 2021)) indicates that a climate-forced signal of increasing breadbasket failures is robust, but our results indicate that it has not yet emerged. The present period of infrequent simultaneous maize breadbasket yield shocks, therefore, may represent an historic period of maize breadbasket stability relative to both the past and future.

In terms of the physical modes of climate variability that affect multiple breadbasket failures, we find that ENSO and the NAO have a large effect on the relative likelihood of simultaneous crop yield shocks in maize and wheat breadbaskets, respectively (see Figs. 6–8). ENSO, the NAO, and the IOD all affect the relative probability of multiple maize or wheat yield shocks in pairs of breadbaskets by up to 20–40%. This effect, however, does not always translate to an increase in the expected number of global wheat or maize breadbaskets experiencing yield shocks (Fig. 9). For example, ENSO increases the probability of wheat yield shocks in some breadbaskets and decreases it in others such that its effect at the global scale is less prominent as compared to its effect on the probability of joint crop yield shocks in pairs of breadbaskets.

The NAO, however, uniformly increases or decreases the probability of joint yield shocks in breadbaskets. As a result, the NAO is the mode of climate variability that most strongly affects the overall number of wheat breadbasket shocks globally. This finding is somewhat surprising provided that the NAO affects cropped areas only in the Northern Hemisphere, while ENSO affects cropped areas globally. The NAO, furthermore, forces both wet and dry precipitation teleconnections. The dissonance between precipitation teleconnections and wheat yield teleconnections is likely because a positive phase of the NAO reduces precipitation in many of the same locations where wheat yields benefit from irrigation, and have done so for nearly a century (Klein et al., 2017; Siebert et al., 2010, 2015; Wang et al., 2021) (SI Fig. 4).

Our analysis relies on subnational and country-level crop statistics, largely collected by national statistics agencies, and departments or ministries of agriculture. There are known systematic errors in statistical data, such as the over-reporting of achievements in China (Liu et al., 2020), and random errors, such as the divergent estimates of crop yields in Malawi reported by the Ministry of Agriculture, the National Census of Agriculture and Livestock, and the Integrated Household Survey conducted by the National Statistics Office ((Carletto et al., 2013). Our approach of taking averages over many years at different yield shock thresholds used in Figs. 6– is designed to mitigate the potential effects of such errors. Likewise, our approach of analyzing changes in the frequency of yield shocks at multiple magnitudes in Figs. 3g,h, 4, and 5 demonstrates the robustness of results across yield thresholds. We furthermore ensure that our results are not due to unreliability of statistical data in the early portion of the data by repeating all the analyses from Figs. 4-9 using the more recent period of 1950–2017, for which the crop yield statistics are more reliable (SI Figures 7–10). The results are robust to this decision. And while establishing statistical significance for some effects in SI Figure 9 is not possible using this shorter time period, the sign and magnitude of results remain similar. Finally, we compare the results of Figs. 6-9 to regional studies on how modes of climate variability affect moisture, temperature, and crop yields to ensure that

our statistical results are consistent with past literature on the dynamics of how ENSO, the IOD, and the NAO affect crop yields.

Overall, our results demonstrate that modes of climate variability, in particular ENSO and the NAO, have large effects on both the pattern and number of simultaneous maize and wheat yield shocks in breadbaskets. We furthermore demonstrate that the frequency of such simultaneous wheat and maize yield shocks has decreased from the 1930s to present despite a modest increase in the frequency of adverse growing conditions. Our ability to continually adapt our food system to a warming world will depend on both the degree of warming and on investments in agricultural research and development. It is critical that we continue to improve our understanding of how both climate change and climate variability affect global breadbaskets as part of those efforts.

Declaration of Competing Interest

The authors declare that they have no known competing financial interests or personal relationships that could have appeared to influence the work reported in this paper.

Data availability

All climate data used in this analysis, including both model output and observational estimates, are publicly available from the sources indicated in the methods section. The crop yield dataset is available from https://sedac.ciesin.columbia.edu/data/set/food-twentieth-century-crop-statistics-1900-2017

Acknowledgments

Weston Anderson would like to acknowledge the mentorship and leadership of Dr. Lisa Goddard during her time as his postdoctoral advisor. Lisa passed away prior to the publication of this work, but was a tireless advocate for building scientific institutions that benefited society and reflected the values of its employees. This work was funded by ACToday, the first of Columbia University's World Projects. All climate data used in this analysis, including both model output and observational estimates, are publicly available from the sources indicated in the methods section. The crop yield data has been deposited with the Socioeconomic Data and Applications Center (SEDAC) and is available from https://sedac.ciesin.columbia.edu/data/set/food-twentieth-century-crop-statistics-1900-2017. All code is available upon request.

Supplementary materials

Supplementary material associated with this article can be found, in the online version, at doi:10.1016/j.agrformet.2023.109321.

References

Anderson, W., Baethgen, W., Capitanio, F., Ciais, P., Rocca da Cunha, G., Goddard, L., Schauberger, B., Sonder, K., Podesta, G., van der Velde, M., You, L., Ru, Y., 2022. Twentieth Century Crop Statistics, 1900-2017. NASA Socioeconomic Data and Applications Center (SEDAC), Palisades, New York. https://doi.org/10.7927/tmsp-sg82. Accessed 10/28/2022.

Anderson, W., Han, E., Baethgen, W., Goddard, L., Muñoz, Á., Robertson, A., 2020. The Madden-Julian Oscillation affects maize yields throughout the tropics and subtropics. Geophys. Res. Lett. 47 (11) e2020GL087 004.

Anderson, W., Seager, R., Baethgen, W., Cane, M., 2017a. Crop production variability in North and South America forced by life-cycles of the El Niño Southern Oscillation. Agric. For. Meteorol. 239, 151–165.

Anderson, W., Seager, R., Baethgen, W., Cane, M., 2017b. Life cycles of agriculturally relevant ENSO teleconnections in North and South America. Int. J. Climatol. 37 (8), 3297–3318.

Anderson, W., Seager, R., Baethgen, W., Cane, M., 2018. Trans-Pacific ENSO teleconnections pose a correlated risk to agriculture. Agric. For. Meteorol. 262, 298–309.

Anderson, W., Seager, R., Baethgen, W., Cane, M., You, L., 2019. Synchronous crop failures and climate-forced production variability. Sci. Adv. 5 (7), eaaw1976.

Baek, S.H., Smerdon, J.E., Coats, S., Williams, A.P., Cook, B.I., Cook, E.R., Seager, R., 2017. Precipitation, temperature, and teleconnection signals across the combined North American, monsoon Asia, and old world drought atlases. J. Clim. 30 (18), 7141–7155.

Cantelaube, P., Terres, J.-M., Doblas-Reyes, F.J., 2004. Influence of climate variability on European agriculture—analysis of winter wheat production. Clim. Res. 27 (2), 135–144.

Caparas, M., Zobel, Z., Castanho, A.D., Schwalm, C.R., 2021. Increasing risks of crop failure and water scarcity in global breadbaskets by 2030. Environ. Res. Lett. 16 (10), 104 013.

Carletto, C., Jolliffe, D., Banerjee, R., 2013. The emperor has no data! agricultural statistics in Sub-Saharan Africa. In: Proceedings of the World Bank Working Paper.

Ceglar, A., Zampieri, M., Gonzalez-Reviriego, N., Ciais, P., Schauberger, B., Van der Velde, M., 2020. Time-varying impact of climate on maize and wheat yields in France since 1900. Environ. Res. Lett. 15 (9), 094039.

Chan, S.C., Behera, S.K., Yamagata, T., 2008. Indian ocean dipole influence on South American rainfall. Geophys. Res. Lett. (14), 35.

Cunha, G., Dalmago, G., Estefanel, V., 2001. El Niño southern oscillation influences on wheat crop in Brazil. Wheat in a Global Environment. Springer, pp. 445–450.

CUNHA, G.R.d., Dalmago, G., Estefanel, V., 1999. ENSO influences on wheat crop in Brazil. Revista Brasileira de Agrometeorologia 7 (1), 127–138.

d'Amour, C.B., Anderson, W., 2020. International trade and the stability of food supplies in the global south. Environ. Res. Lett. 15 (7), 074 005.

d'Amour, C.B., Wenz, L., Kalkuhl, M., Steckel, J.C., Creutzig, F., 2016. Teleconnected food supply shocks. Environ. Res. Lett. 11 (3), 035 007.

Fischer, G., M. Shah, H. Van Velthuizen, and F.O. Nachtergaele, 2001: Global agro-ecological assessment for agriculture in the 21st century.

Funk, C., et al., 2018. Examining the role of unusually warm Indo-Pacific sea-surface temperatures in recent African droughts. Q. J. R. Meteorolog. Soc. 144, 360–383.

Gaupp, F., Hall, J., Hochrainer-Stigler, S., Dadson, S., 2020. Changing risks of simultaneous global breadbasket failure. Nat Clim Chang 10 (1), 54–57.

Gaupp, F., Hall, J., Mitchell, D., Dadson, S., 2019. Increasing risks of multiple breadbasket failure under 1.5 and 2C global warming. Agric. Syst. 175, 34–45.

Goddard, L., Graham, N.E., 1999. Importance of the Indian Ocean for simulating rainfall anomalies over Eastern and Southern Africa. J. Geophys. Res. 104 (D16), 19 099–19 116.

Handler, P., 1984. Corn yields in the United States and sea surface temperature anomalies in the equatorial Pacific Ocean during the period 1868–1982. Agric. For. Meteorol. 31 (1), 25–32.

Hasegawa, T., Wakatsuki, H., Nelson, G.C., 2022. Evidence for and projection of multi-breadbasket failure caused by climate change. Curr. Opin. Environ. Sustain. 58 (101), 217.

Hastie, T., Tibshirani, R.I., 2009. The Elements of Statistical learning: Data mining, inference, and Prediction/By Trevor Hastie, Robert Tibshirani, Jerome Frieman. Springer.

Heslin, A., et al., 2020. Simulating the cascading effects of an extreme agricultural production shock: global implications of a contemporary US Dust Bowl event. Front. Sustain. Food Syst. 4, 26.

Hurrell, J.W., 1995. Decadal trends in the North Atlantic Oscillation: regional temperatures and precipitation. Science 269 (5224), 676–679.

Iizumi, T., Luo, J.-J., Challinor, A.J., Sakurai, G., Yokozawa, M., Sakuma, H., Brown, M. E., Yamagata, T., 2014. Impacts of El Niño Southern Oscillation on the global yields of major crops. Nat. Commun. 5 (May), 3712. https://doi.org/10.1038/ncomms4712. URL. http://www.ncbi.nlm.nih.gov/pubmed/24827075.

Jägermeyr, J., et al., 2021. Climate impacts on global agriculture emerge earlier in new generation of climate and crop models. Nat. Food 2 (11), 873–885.

Jain, M., et al., 2021. Groundwater depletion will reduce cropping intensity in india. Sci. Adv. 7 (9), eabd2849.

Janetos, A., C. Justice, M. Jahn, M. Obersteiner, J. Glauber, and W. Mulhern, 2017: The Risks of Multiple Breadbasket Failures in the 21st century: a Science Research Agenda. Boston University Frederick S. Pardee Center for the Study of the Longer-Range Future.

Kent, C., Pope, E., Thompson, V., Lewis, K., Scaife, A.A., Dunstone, N., 2017. Using climate model simulations to assess the current climate risk to maize production. Environ. Res. Lett. 12 (5), 054 012.

Klein Goldewijk, K., Beusen, A., Doelman, J., Stehfest, E., 2017. Anthropogenic land use estimates for the Holocene–Hyde 3.2. Earth Syst. Sci. Data 9 (2), 927–953.

Kornhuber, K., Coumou, D., Vogel, E., Lesk, C., Donges, J.F., Lehmann, J., Horton, R.M., 2020. Amplified Rossby waves enhance risk of concurrent heatwaves in major breadbasket regions. Nat. Clim. Chang. 10 (1), 48–53.

Lamb, P.J., Peppler, R.A., 1987. North atlantic oscillation: concept and an application. Bull. Am. Meteorol. Soc. 68 (10), 1218–1225.

Lesk, C., Anderson, W., 2021. Decadal variability modulates trends in concurrent heat and drought over global croplands. Environ. Res. Lett. 16 (5), 055 024.

Liu, B., et al., 2019. Global wheat production with 1.5 and 2.0◦ c above pre-industrial warming. Glob. Chang Biol. 25 (4), 1428–1444.

Liu, G., et al., 2020. On the accuracy of official chinese crop production data: evidence from biophysical indexes of net primary production. Proc. Natl. Acad. Sci. 117 (41), 25 434–25 444.

Liu, W., Ye, T., Jägermeyr, J., Müller, C., Chen, S., Liu, X., Shi, P., 2021. Future climate change significantly alters interannual wheat yield variability over half of harvested areas. Environ. Res. Lett. 16 (9), 094 045.

Liu, Y., Yang, X., Wang, E., Xue, C., 2014. Climate and crop yields impacted by ENSO episodes on the North China Plain: 1956–2006. Reg. Environ. Change 14 (1), 49–59.

Lybbert, T.J., Smith, A., Sumner, D.A., 2014. Weather shocks and inter-hemispheric supply responses: implications for climate change effects on global food markets. Clim. Change Econ. 5 (04), 1450 010.
Maignan, F., Bréon, F.-M., Bacour, C., Demarty, J., Poirson, A., 2008. Interannual vegetation phenology estimates from global AVHRR measurements: comparison with in situ data and applications. Remote Sens. Environ. 112 (2), 496–505.
Marchand, P., et al., 2016. Reserves and trade jointly determine exposure to food supply shocks. Environ. Res. Lett. 11 (9), 095 009.
Mauget, S.A., Upchurch, D.R., 1999. El Niño and La Niña related climate and agricultural impacts over the Great Plains and Midwest. J. Product. Agric. 12 (2), 203–215.
Mehrabi, Z., Ramankutty, N., 2019. Synchronized failure of global crop production. Nat. Ecol. Evol. 3 (5), 780–786.
Najafi, E., Pal, I., Khanbilvardi, R., 2020. Larger-scale ocean-atmospheric patterns drive synergistic variability and world-wide volatility of wheat yields. Sci. Rep. 10 (1), 1–11.
Páscoa, P., Gouveia, C., Russo, A., Trigo, R., 2017. Drought trends in the Iberian Peninsula over the last 112 years. Adv. Meteorol. **2017**.
Podestá, G.P., Messina, C.D., Grondona, M.O., Magrin, G.O., 1999. Associations between grain crop yields in Central-Eastern Argentina and El Niño-Southern Oscillation. J. Appl. Meteorol. 38 (10), 1488–1498. https://doi.org/10.1175/1520-0450(1999)038<1488:ABGCYI>2.0.CO;2.
Portmann, F.T., Siebert, S., Döll, P., 2010. Mirca2000—global monthly irrigated and rainfed crop areas around the year 2000: a new high-resolution data set for agricultural and hydrological modeling. Global Biogeochem. Cycles 24 (1).
Porkka, M., Kummu, M., Siebert, S., Varis, O., 2013. From food insufficiency towards trade dependency: a historical analysis of global food availability. PLoS One 8 (12) e82 714.
Proctor, J., Rigden, A., Chan, D., Huybers, P., 2022. More accurate specification of water supply shows its importance for global crop production. Nat. Food 3 (9), 753–763.
Puma, M.J., Bose, S., Chon, S.Y., Cook, B.I., 2015. Assessing the evolving fragility of the global food system. Environ. Res. Lett. 10 (2), 024 007.
Raymond, C., Suarez-Gutierrez, L., Kornhuber, K., Pascolini-Campbell, M., Sillmann, J., Waliser, D.E., 2022. Increasing spatiotemporal proximity of heat and precipitation extremes in a warming world quantified by a large model ensemble. Environ. Res. Lett. 17 (3), 035 005.
Rayner, N.A.A., Parker, D.E., Horton, E.B., Folland, C.K., Alexander, L.V., Rowell, D.P., Kent, E.C., Kaplan, A., 2003. Global analyses of sea surface temperature, sea ice, and night marine air temperature since the late nineteenth century. J. Geophys. Res. 108 (D14).
Rigden, A., Mueller, N., Holbrook, N., Pillai, N., Huybers, P., 2020. Combined influence of soil moisture and atmospheric evaporative demand is important for accurately predicting us maize yields. Nat. Food 1 (2), 127–133.
Rodell, M., Houser, P., Jambor, U., Gottschalck, J., et al., 2004. The global land data assimilation system. Bull. Am. Meteorol. Soc. 85 (3), 381.
Rohde, R., et al., 2013. Berkeley earth temperature averaging process. Geoinfo. Geostat. 1 (2), 1–13.
Sacks, W.J., Deryng, D., Foley, J.A., Ramankutty, N., 2010. Crop planting dates: an analysis of global patterns. Global ecology and biogeography 19 (5), 607–620.
Sánchez, B., Rasmussen, A., Porter, J.R., 2014. Temperatures and the growth and development of maize and rice: a review. Glob Chang. Biol. 20 (2), 408–417.
Sarhadi, A., Ausín, M.C., Wiper, M.P., Touma, D., Diffenbaugh, N.S., 2018. Multidimensional risk in a nonstationary climate: joint probability of increasingly severe warm and dry conditions. Sci. Adv. 4 (11), eaau3487.
Schauberger, B., Ben-Ari, T., Makowski, D., Kato, T., Kato, H., Ciais, P., 2018. Yield trends, variability and stagnation analysis of major crops in France over more than a century. Sci. Rep. 8 (1), 1–12.
Schauberger, B., Kato, H., Kato, T., Watanabe, D., Ciais, P., 2022. French crop yield, area and production data for ten staple crops from 1900 to 2018 at county resolution. Sci. Data 9 (1), 1–6.
Schillerberg, T.A., Tian, D., 2020. Changes of crop failure risks in the United States associated with large-scale climate oscillations in the Atlantic and Pacific Oceans. Environ. Res. Lett. 15 (6), 064035.
Schlenker, W., Roberts, M.J., 2009. Nonlinear temperature effects indicate severe damages to us crop yields under climate change. Proc. Natl. Acad. Sci. 106 (37), 15 594–15 598.
Selvaraju, R., 2003. Impact of El Niño–Southern Oscillation on Indian foodgrain production. Int. J. Climatol. 23 (2), 187–206.
Siebert, S., Burke, J., Faures, J.-M., Frenken, K., Hoogeveen, J., Döll, P., Portmann, F.T., 2010. Groundwater use for irrigation–a global inventory. Hydrol. Earth Syst. Sci. 14 (10), 1863–1880.
Siebert, S., Kummu, M., Porkka, M., Döll, P., Ramankutty, N., Scanlon, B.R., 2015. A global data set of the extent of irrigated land from 1900 to 2005. Hydrol. Earth Syst. Sci. 19 (3), 1521–1545.
Singh, D., Seager, R., Cook, B.I., Cane, M., Ting, M., Cook, E., Davis, M., 2018. Climate and the global famine of 1876–78. J. Clim. 31 (23), 9445–9467.
Tian, D., Asseng, S., Martinez, C.J., Misra, V., Cammarano, D., Ortiz, B.V., 2015. Does decadal climate variation influence wheat and maize production in the southeast USA? Agric. For. Meteorol. 204, 1–9.
Tigchelaar, M., Battisti, D.S., Naylor, R.L., Ray, D.K., 2018. Future warming increases probability of globally synchronized maize production shocks. Proc. Natl. Acad. Sci. 115 (26), 6644–6649.
Timmermann, A., et al., 2018. El Niño–Southern Oscillation complexity. Nature 559 (7715), 535–545.
Toreti, A., Cronie, O., Zampieri, M., 2019. Concurrent climate extremes in the key wheat producing regions of the world. Sci. Rep. 9 (1), 1–8.
Trnka, M., et al., 2016. Changing regional weather crop yield relationships across Europe between 1901 and 2012. Clim. Res. 70 (2–3), 195–214.
Ummenhofer, C.C., England, M.H., McIntosh, P.C., Meyers, G.A., Pook, M.J., Risbey, J.S., Gupta, A.S., Taschetto, A.S., 2009. What causes southeast Australia's worst droughts? Geophys. Res. Lett. 36 (4).
van der Schrier, G., Barichivich, J., Briffa, K., Jones, P., 2013. A scPDSI-based global data set of dry and wet spells for 1901–2009. J. Geophys. Res. 118 (10), 4025–4048.
Wang, X., et al., 2021. Global irrigation contribution to wheat and maize yield. Nat. Commun. 12 (1), 1–8.
Wittenberg, A.T., 2009. Are historical records sufficient to constrain ENSO simulations? Geophys. Res. Lett. 36 (12).
You, L., Wood, S., Wood-Sichra, U., Wu, W., 2014. Generating global crop distribution maps: from census to grid. Agric. Syst. 127, 53–60.
Yuan, C., Yamagata, T., 2015. Impacts of IOD, ENSO and ENSO Modoki on the Australian winter wheat yields in recent decades. Sci. Rep. 5 (1), 1–8.
Zampieri, M., Ceglar, A., Dentener, F., Dosio, A., Naumann, G., Van Den Berg, M., Toreti, A., 2019. When will current climate extremes affecting maize production become the norm? Earth's Future 7 (2), 113–122.